The periodic table shape possible to coincide with a proton distribution

Jianping Mao

201-A-22 Qinye Changzhou, Jiangsu 213016, China
E-mail: mjp00951@163.com

Abstract

The periodic table shape seems to coincide with a folding crystal structure of atomic nuclei, an orderly distribution of protons (nucleons) nearly the same as Lewis dot structure, which will grow vertical 4 A (representative), 4 B (transition) and 8 C (inner transition) α-clusters bound with valence neutrons (excess neutrons, ~ $A - 2Z$) to stand a core (1st period) of likely expanding in Co, Ni, Rh and Pd. In a typical fission of $^{235}U+n \rightarrow {}^{137}Ba+{}^{97}Kr+2n$, ^{137}Ba and ^{97}Kr mass difference is suggested to result from the 16 α-clusters cleft into 9:7 ($\pm$1 A α-cluster, 5 α $\times$ 2 = 40) and 2n release from valence neutrons in its cleft line; also, cleft into 15:1 implies to point to that α-cluster (1 C $\geqslant {}^{4}He$, 1 B $\geqslant {}^{12}C$, 1 A $\geqslant {}^{20}Ne$) decay. To cross nuclei, atoms and molecules, here a way may enable us closer to nature of the periodic table, the periodic law of dominating their behaviors.

Keywords: periodic table, proton distribution, valence neutron, nuclear core, α-cluster decay, nuclear fission

PACS:

01.30.Kj Handbook, dictionaries, tables, and data compilations

21.10.Dr Binding energies and masses

21.10.Ft Charge distribution

21.10.Gv Nucleon distributions and halo features

21.60.-n Nuclear structure models and methods

21.60.Gx Cluster models

23.35.+g Isomer decay

23.60.+e α decay

23.70.+j Heavy-particle decay

24.75.+I General properties of fission

32.10.-f Properties of atoms

33.15.-e Properties of molecules

Contents:

1. Introduction

The periodic table with the elements accumulated now is well-known and plays a guide role in physical science. Its shape, *Z*, the atomic number, the periodic law, is currently explained by the electron since it is discovered (1) to establish atomic models (2-4), an atomic periodicity, though about in the same time it has been proven to result from the proton number (5, 6). This seems possible to attribute to that a clear cubic distributions of *Z* in a nucleus (7) consisting of protons and neutrons (8) might has not been revealed (9-11), to the best of the author's knowledge. However, it may be a flaw to ignore Moseley's work (5, 6) that the proton number could convey a nuclear periodicity to a certain extent. As the shell model (11), its magic nuclei 2, 8, 20, 28, 50, 82 and 126 is apparently inconsistent with noble nuclei (gases) 2, 10, 18, 36, 54, 86 and 118, while noble nuclei appear to close naturally that could display a cubic *Z* in a tangible proton distributions. It was observed in analysis molecular structure, crossing nuclear, atomic and molecular three levels, which is both quite simple and universal.

The observation is starting from a curiosity that whether an atomic mass has an influence upon molecular bond energy or not about in the summer of 1987. Because an element occurs some isotopes and then had no intention of taking their relative mass what want to see nucleons how to distribute in a molecule (atom), every element is represented by its maximal abundant isotope (Table 1) selected from a handbook (*U.S. National Nuclear Data Center. "NuDat 2.6"* and *"It's Elemental"*.). The simulation of nucleon distributions of atoms in a molecule is that according to their number of periods and groups. For instance, in $^{12}C^{1}H_4$, their isotopic masses marked in the molecular formula, ^{1}H (99.9%, natural abundance) is clear; ^{12}C (98.9%) is in the 2nd period and group 4A, indicating that its 6 p should be separated into: 2 p in nuclear core and 4 p in nuclear skin, then its 6 n overlap this 6 p frame, that is, $^{12}C_{c\text{-}2+2}{}^{2222}$ (most notes in captions of Table 1, Figs. 1*A-C* and 2*A*), which is a tetrahedral distribution to connect 4 ^{1}H atoms, a $^{12}C^{1}H_4$ molecular-nuclear (M-N) structure (Supporting fig. S122), as it is well-known that a methane is a tetrahedral structure. Also, it seems to be straightforward that if alternating single and double bonds of a benzene ring ($^{12,13,14}C_6{}^{1}H_6$, fig. S125), a buckyball ($^{12,13,14}C_{60}$) and diamond ($^{12,13,14}C_n$) are rooted in a tetrahedral nucleus of $^{12,13,14}C$. Here, black and white stones of Go (a game) were used to stand for protons and neutrons, respectively. It is useful in this early work; without it is difficult to simulate a M-N structure, nuclear structure and fission, since a nucleus is a system of numerous nucleons.

In order to test, this proton distribution, which could be regarded as nucleon distributions for that neutrons by and large surround protons to fit in a nucleus, is used trying to account for nuclear fission phenomena (12): structures, mass difference and vanishing points of fragments, released neutrons, and emission angle of fission α-particles. Furthermore, it implies that both α and cluster (heavy-particle, mass $A > 4$) decay are similar to fission in principle that only mass ratios are different. Now first is to describe this nuclear crystal model, a nucleon distribution like a crystal (Figs. 2*A-B*), which seems to coincide with the periodic law that periods and groups of the periodic table are corresponding to horizontal 7 layers and vertical 16 α-clusters of nuclei, respectively (Figs. 1*A-C* and 2*A*). In the 1, 2-3, 4-5 and 6-7 periods/layers or nuclear 0, A, B and C 4 steps, respectively, basic, light, mid and heavy nuclei will be exhibited in crystal growth of nuclei (Table 1 or figs. S1-118) to pose different shapes that imply to be folding, seemingly somewhat corresponding to nuclear deformation.

Fig. 1. Nuclear folded and unfolded frames.

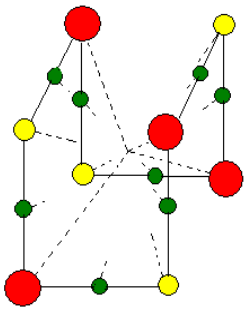

A

	5B				16C	8C	5A	1A		1C	9C				2B		
1B		107			102	94	115	87		103	95			112		6B	
	111		75		70	62	83	55		71	63		80		108		
		79		41			51	37				48		76			
			47		23		33	19			30		42				
7C	93	61		29			15	11				24		72	104	2C	
15C	101	69					7	3						64	96	10C	
								1									
4A	114	82	50	32	14	6		27	28		8	16	34	52	84	116	6A
8A	118	86	54	36	18	10	2	45	46		4	12	20	38	56	88	2A
									1								
6C	92	60					5	9	2						65	97	11C
14C	100	68		22			13	17	3			25		57	89	3C	
			40		26		31	35	4		21		43				
		74		44			49	53	5			39		77			
	106		78		59	67	81	85	6	58	66		73		109		
4B		110			91	99	113	117	7	90	98			105		7B	
	8B				5C	13C	3A	7A		4C	12C				3B		

B

	1A	2A	3B	4B	5B	6B	7B	8B	9B	10B	1B	2B	3A	4A	5A	6A	7A	8A
1	1																	2
2	3	4											5	6	7	8	9	10
3	11	12											13	14	15	16	17	18
4	19	20	21	22	23	24	25	26	27	28	29	30	31	32	33	34	35	36
5	37	38	39	40	41	42	43	44	45	46	47	48	49	50	51	52	53	54
6	55	56	73	74	75	76	77	78			79	80	81	82	83	84	85	86
7	87	88	105	106	107	108	109	110			111	112	113	114	115	116	117	118

3C	4C	5C	6C	7C	8C	9C	10C	11C	12C	13C	14C	15C	16C	1C	2C
57	58	59	60	61	62	63	64	65	66	67	68	69	70	71	72
89	90	91	92	93	94	95	96	97	98	99	100	101	102	103	104

C

(*A*) Nuclei seem to grow 4 A ($Z \geqslant 10$, red), 4 B ($Z \geqslant 26$, yellow) and 8 C ($Z \geqslant 70$, green) α-clusters (axes), where are ^{l}p (last proton, added to the prior element, $Z - 1$) locations of A (representative), B (transition) and C (inner transition) family elements, respectively. (*B*) Growing locations of ^{l}p of Z 1-118. The period is in the middle (uncolored) and the group is in four sides. The groups 1A, 5A pair on A1 axis, and so on; it is the same way for the B and C family groups. Four ^{l}p of $Z = 27$, 28, 45 and 46 in old group 8B (American convention; groups 8-10, modern form), which was revised into groups 8-10B, are sunk into the 1st period. (*C*) The A (red), B (yellow) and C (green) families correspond to 4 A, 4 B and 8 C α-clusters, respectively. As 8 C α-clusters occupy 16 ^{l}p, the number of C family elements is suggested to increase from 2×14 to 2×16, then group 8B only leave $_{78}$Pt and $_{110}$Ds. The classification of C family is following previous B family that $_{71}$Lu and $_{72}$Hf of groups 1-2C into inner transition is analogous to $_{29}$Cu and $_{30}$Zn of groups 1-2B into transition, though C shell has right been closed at $_{70}$Yb in Table 1.

Table 1. A periodic distributions of nucleons for the maximal abundant isotopes.

In expression of nucleon distributions, subscript, left and right superscript of the periodic number are the numbers of ^{v}n, ^{p}n and ^{l}p respectively, and skins are axial configurations that 4 A, 4 B and 8 C axes in 7 codes (the Arabic numeral): 1, proton (p); 2, deuteron (d); 3, triton (t); 4, alpha particle (α); 0, neutron (n); 2̲, di-neutrons (^{d}n); 3̲, ^{3}He ion. Hyphen (-) is the same as upside. Chemical valence corresponding to axial configuration is listed in the 2nd period. In the 3rd period is grown mass between these nuclei. There will be a fluctuation only if ^{58}Ni (67.88%) and ^{106}Pd (27.33%) in group 10B are listed.

nucleus	nucleon distribution	chemical valence (^{1,2,3}H)	grown mass	abundance (%) / half-life
^{1}H	1^{a-1}			99.9
^{4}He	1^{a-1010}			100
^{7}Li	$^{2}1^{2}$ 2^{a-100}	1		92.4
^{9}Be	- 2^{a-2010}	2		100
^{11}B	- 2^{a-0222}	3		80.1
^{12}C	- 2^{a-2222}	4		98.9
^{14}N	- 2^{a-4222}	3		99.6
^{16}O	- 2^{a-4242}	2		99.7
^{19}F	- 2^{a-4443}	1		100
^{20}Ne	- 2^{a-4444}	0		90.4
^{23}Na	- $^{8}2^{8}$ 3^{a-100}			100
^{24}Mg	- - 3^{a-1010}		1	78.9
^{27}Al	- - 3^{a-0222}		3	100
^{28}Si	- - 3^{a-2222}		1	92.2
^{31}P	- - 3^{a-4232}		3	100
^{32}S	- - 3^{a-4242}		1	94.9
^{35}Cl	- - 3^{a-4443}		3	75.7
^{40}Ar	- - $_{4}3^{a-4444}$		5	99.6
^{39}K	- - $^{8}3^{8}$ 4^{a-100}			93.3
^{40}Ca	- - - 4^{a-1010}			96.9
^{45}Sc	- - $^{8}_{4}3^{8}$ $4^{b-111\underline{2}}$			100
^{48}Ti	- - - 4^{b-2222}			73.7
^{51}V	- - - 4^{b-4232}			99.7
^{52}Cr	- - - 4^{b-4242}			83.7
^{55}Mn	- - - 4^{b-4443}			100
^{56}Fe	- - - 4^{b-4444}			91.7
^{59}Co	$^{4}1^{3}$ - - 4 -			100
^{60}Ni	$^{4}1^{4}$ - - 4 -			26.2
^{63}Cu	- - - 4 - $^{a-100}$			69.1
^{64}Zn	- - - 4 - $^{a-1010}$			49.1
^{69}Ga	- - - $_{4}4$ - $^{a-111\underline{2}}$			60.1
^{74}Ge	- - - $_{4}4$ - $^{a-3232}$			36.5
^{75}As	- - - $_{4}4$ - $^{a-4232}$			100
^{80}Se	- - - $_{8}4$ - $^{a-4242}$			49.6
^{79}Br	- - - $_{4}4$ - $^{a-4443}$			50.6
^{84}Kr	- - - $_{8}4$ - $^{a-4444}$			56.9

^{85}Rb	-	-	-	$^{16}_{8}4^{16}$	5	a-1					72.1
^{88}Sr	-	-	-	-	5	a-1010					82.5
^{89}Y	-	-	$^{8}3^{8}$	-	5	b-1112	a-0000				100
^{90}Zr	-	-	-	-	5	b-1212	-				51.4
^{93}Nb	-	-	-	-	5	b-4333					100
^{98}Mo	-	-	-	-	5	b-4343	a-0000				24.3
^{99}Tc	-	-	-	-	5	b-4443	-				2.1×10^{5} yr
^{102}Ru	$^{6}1^{4}$	-	-	-	5	b-4444	-				31.5
^{103}Rh	$^{6}1^{5}$	-	-	-	5	-	-				100
^{104}Pd	$^{6}1^{6}$	-	-	-	5	-	-				11.1
^{107}Ag	-	-	-	-	5	-	a-1222				51.8
^{114}Cd	-	$^{8}_{4}2^{8}$	$^{8}_{4}3^{8}$	-	5	-	a-1122				28.7
^{115}In	-	-	-	-	5	-	a-0222				95.7
^{120}Sn	-	-	-	-	5	-	a-3333				32.5
^{121}Sb	-	-	-	-	5	-	a-4333				57.2
^{130}Te	-	-	-	-	$_{8}5$	-	a-4343				34.08
^{127}I	-	-	-	-	$_{4}5$	-	a-4443				100
^{132}Xe	-	-	-	-	$_{8}5$	-	a-4444				26.9
^{133}Cs	-	-	-	-	$^{16}_{8}5^{16}$	6	a-1				100
^{138}Ba	-	-	-	-	-	6	a-1122				71.6
^{139}La	-	-	-	-	$^{16}5^{16}$	6	c-1010-100	b-0000	a-0000		99.9
^{140}Ce	-	-	-	-	-	6	c-1010-1010	-	-		88.4
^{141}Pr	-	-	-	-	-	6	c-1010-1112	-	-		100
^{142}Nd	-	-	-	-	-	6	c-1112-1112	-	-		27.1
^{145}Pm	-	-	-	-	-	6	c-2121-2122	-	-		17.7 yr
^{152}Sm	-	-	-	-	-	6	c-3232-3232	-	-		26.7
^{153}Eu	-	-	-	-	-	6	c-4232-3232	-	-		52.1
^{158}Gd	-	-	-	-	-	6	c-4333-4333	-	-		24.8
^{159}Tb	-	-	-	-	-	6	c-4343-4333	-	-		100
^{164}Dy	-	$^{8}2^{8}$	-	-	$^{16}_{8}5^{16}$	6	c-4343-4343	-	-		28.2
^{165}Ho	-	-	-	-	-	6	c-4443-4343	-	-		100
^{166}Er	-	-	-	-	-	6	c-4443-4443	-	-		33.5
^{169}Tm	-	-	-	-	-	6	c-4444-4443	b-0022	-		100
^{174}Yb	-	$^{8}_{4}2^{8}$	-	-	-	6	c-4444-4444	-	-		32.02
^{175}Lu	-	-	-	-	-	6	-	b-1222	-		97.4
^{180}Hf	-	-	-	-	-	6	-	b-2222	a-2222		35.08
^{181}Ta	-	-	-	-	-	6	-	b-3222	-		99.9
^{184}W	-	-	-	-	-	6	-	b-3333	-		30.6
^{187}Re	-	-	-	-	-	$_{2}6$	-	b-4333	-		62.6
^{192}Os	-	-	-	-	-	$_{6}6$	-	b-4343	-		40.7
^{193}Ir	-	-	-	-	-	$_{6}6$	-	b-4443	-		62.7
^{194}Pt	-	-	-	-	-	$_{6}6$	-	b-4444	-		32.8
^{197}Au	-	-	-	-	-	$_{10}6$	-	-	a-1222		100
^{202}Hg	-	-	-	-	-	$_{16}6$	-	-	a-1122		29.8
^{205}Tl	-	-	-	-	-	$_{16}6$	-	-	a-2232		70.4
^{208}Pb	-	-	-	-	-	$_{16}6$	-	-	a-3333		52.4

^{209}Bi	-	-	-	-	-	$_{16}6$ - - a-4333		100
^{209}Po	-	-	-	-	-	$_{16}6$ - - a-4342		102 yr
^{210}At	-	-	-	-	-	$_{16}6$ - - a-4442		8.1 h
^{222}Rn	$^{6}{}_{6}1^{6}$	-	-	-	-	$_{16}6$ - - a-4444	$^{4}7$	3.82 d
^{223}Fr	-	-	-	-	-	$^{32}{}_{16}6^{32}$	7 b-0000 a-1	22 min
^{226}Ra	-	-	-	-	-	-	7 - a-1010	1600 yr
^{227}Ac	$^{6}1^{6}$	-	-	-	-	-	$7^{c-1010-100}$ - a-0000	21.77 yr
^{232}Th	-	-	-	-	-	-	$7^{c-11\underline{22}-11\underline{22}}$ - -	1.4×10^{10} yr
^{231}Pa	-	-	-	-	-	-	$7^{c-11\underline{22}-111\underline{2}}$ - -	3.3×10^{4} yr
^{238}U	-	-	-	-	-	-	$7^{c-333\underline{2}-333\underline{2}}$ - -	99.2
^{237}Np	-	-	-	-	-	-	$7^{c-2223-222\underline{2}}$ - -	2.1×10^{6} yr
^{244}Pu	-	-	-	-	-	-	$7^{c-3333-3333}$ - -	8.0×10^{7} yr
^{243}Am	-	-	-	-	-	-	$7^{c-4323-3323}$ - -	7370 yr
^{247}Cm	-	-	-	-	-	-	$7^{c-4323-4322}$ b-$\underline{2222}$ -	1.56×10^{7} yr
^{247}Bk	-	-	-	-	-	-	$7^{c-4242-4322}$ - -	1.38×10^{3} yr
^{251}Cf	-	-	-	-	-	-	$7^{c-4343-4342}$ - -	898 yr
^{252}Es	-	-	-	-	-	-	$7^{c-4443-4342}$ - -	471.7 d
^{257}Fm	-	-	-	-	-	-	$7^{c-4443-4442}$ - a-$\underline{2222}$	100.5 d
^{258}Md	-	-	-	-	-	-	$7^{c-4444-4442}$ - -	51.5 d
^{259}No	-	-	-	-	-	-	$7^{c-4444-4444}$ b-0$\underline{222}$ -	58 min
^{260}Lr	-	-	-	-	-	-	7 - b-2$\underline{222}$ -	3 min
^{261}Rf	-	-	-	-	-	-	7 - b-32$\underline{22}$ -	1.9 s
^{262}Db	-	-	-	-	-	-	7 - b-233$\underline{2}$ -	35 s
^{265}Sg	-	-	-	-	-	-	$_{1}7$ - b-3333 -	16.2 s
^{272}Bh	-	-	-	-	-	-	$_{7}7$ - b-4333 -	10 s
^{275}Hs	-	-	-	-	-	-	$_{9}7$ - b-4343 -	0.15 s
^{276}Mt	-	-	-	-	-	-	$_{9}7$ - b-4443 -	0.72 s
^{281}Ds	-	-	-	-	-	-	$_{16}7$ - b-4444 a-$\underline{2}$000	20 s
^{281}Rg	-	-	-	-	-	-	$_{16}7$ - - a-2000	26 s
^{285}Cn	-	-	-	-	-	-	$_{16}7$ - - a-32$\underline{22}$	30 s
^{286}113	-	-	-	-	-	-	$_{16}7$ - - a-323$\underline{2}$	20 s
^{288}114	-	-	-	-	-	-	$_{16}7$ - - a-3333	0.52 s
^{289}115	-	-	-	-	-	-	$_{16}7$ - - a-4333	0.22 s
^{290}116	-	-	-	-	-	-	$_{16}7$ - - a-4343	15 ms
^{291}117	-	-	-	-	-	-	$_{16}7$ - - a-4443	
^{292}118	$^{6}1^{6}$	$_{4}2^{a-4444}$	$_{4}3^{a-4444}$	$_{8}4^{b-4444\ a-4444}$	$_{8}5^{b-4444\ a-4444}$	$_{16}6^{c-4444-4444\ b-4444\ a-4444}$	$_{16}7^{c-4444-4444\ b-4444\ a-4444}$	

2. Nuclear 4 steps and 16 α-clusters

2.1. The 1st period: nuclear core. Atomic nuclei appear to consist of 7 kind of particles: ^{1,2,3}H, ^{3,4}He, valence neutron and di-neutrons (unclear who termed), which can be separated into core, middle and skin three parts, core+middle = ^{m}c ($Z \geqslant 11$); skin mass, ^{m}s, its particle structures and distributions was called axial configuration in ground state. Collectively, ^{m}c is a noble nucleus and core is a ^{4}He of the closed 1st period in a range Z = 3-26, for it will expand in Z = 27, where Z = 21, 27 and 57 are three key points in proton distributions, implying to differ from prevailing electron

distributions (configurations). On the other hand, in nuclear growth a nucleon behavior seems to loom up a tetrahedral shape having some "nucleon valence" (~ 4) to bind other nucleons or basic nuclei (Fig. 2*A*) with an explicit direction, suggesting that a molecular bond may result essentially from this character (Fig. 2*B*). Figures. 2*A*-*B* also support a view that a nucleus and a molecule able to be a three dimensional structure depend largely on that an α-particle is tetrahedral, a most concise solid structure in nature.

Fig. 2. A crystal images of ^{208}Pb (unfolded) and $^{1}H_2{}^{16}O$.

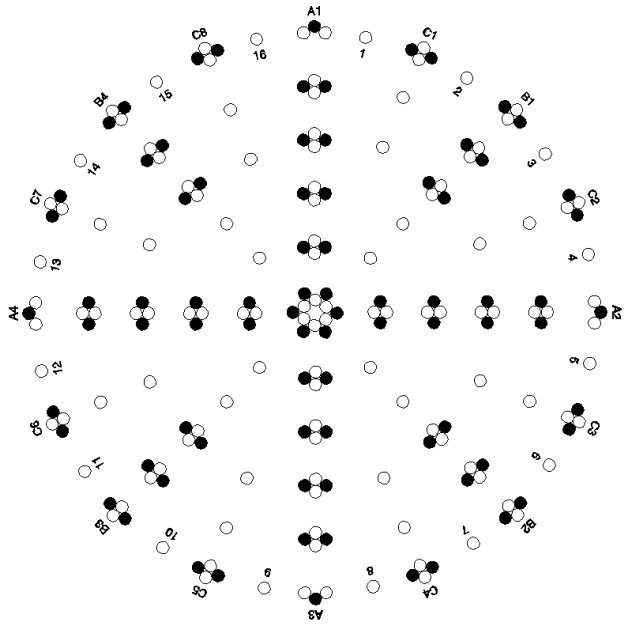

A

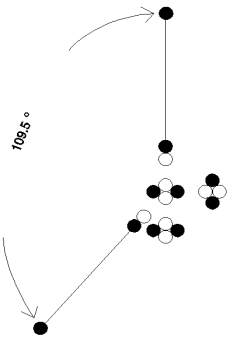

B

(*A*) Closed and open circles are protons and neutrons, respectively. In $^{208}{}_{82+86+40}Pb_{c\text{-}6+6,v\text{-}40}{}^{c\text{-}4444\text{-}4444,b\text{-}4444,a\text{-}3333}$, right superscript is axial configuration, subscript c-6+6 is core (n+p), v-40 is ^{v}n number and 82+86+40 is $Z+^{p}n+^{v}n$ three frames (shells), where ^{p}n is pair neutron accompanying proton to form ^{2,3}H and ^{3,4}He, and ^{v}n is valence neutron (single open circles) to fill gaps in axes and layers. In order to describe fission, a nuclear coordinate was introduced that the serial numbers of axes and layers are after A, B and C letters; for valence neutron is N that it is clockwise rotating from A1 axis to the origin point: 1→4, 1→8 and 1→16 in A, B and C steps, respectively. This figure suggests that in 1-1/4-8 fission (from N1-6 through 1/4 core to N8-6), 1-8 and 8-1 sectors are light (A_L) and heavy (A_H) fragments, respectively (21-23), some of 6 ^{v}n (N1-6, 1-4, 1-2 and N8-6, 4-4, 2-2) are become free neutrons (24, 25) in the cleft line, and angular distributions of α-particle (26, 27) are 90 - 22.5° for A_L and 90+22.5° for A_H coming from C1-6 or C4-6. (*B*) In the center of $^{1}H_2{}^{16}O$ is a $^{16}O_{c\text{-}2+2}{}^{4242}$ and the farthest are 2 ^{1}H, suggesting that its chemical valence and their angle are rooted in 2 d on the nuclear skin. If the 2 d of $^{16}O^{4242}$ (99.757%) were replaced by 1 or 2 t, it is $^{17}O^{4342}$ (0.038%) or $^{18}O^{4343}$ (0.205%).

2.2. The 2-3 periods: Lewis dot structure of nuclear skin. In F_2, O_2 and N_2 molecules, a single, a double and a triple bond coincided with a pair of t in two nuclear skins of $(^{19}F^{4443})_2$, two pairs of d in $(^{16}O^{4242})_2$ and three pairs of d in $(^{14}N^{4222})_2$ suggest that molecular different shapes may be rooted in axial configurations (see also figs. S119-124: $^{23}Na^{35}Cl$, $^{9}Be^{35}Cl_2$, $^{11}B^{19}F_3$, $^{12}C^{1}H_4$, $^{14}N_2$ and $^{16}O_3$, respectively). In the 2nd layer, nuclei start to grow up to 4 α-particles (8 elements) standing on 4 nucleons of a basal tetrahedral α-particle. In $^{7}Li_{c\text{-}2+2}{}^{100}$, axial configuration is a-100 that its 1 ^{l}p with 2 ^{p}n are dispersed on 3 axes of 4 hole axes, thus its skin has merely a proton in that molecular structure is reflected 1 of chemical valence. Generally, the number is equal between chemical main valence and ^{1,2,3}H (p, d and t) at top of nuclear 4 A axes (Table 1), which is nearly the same as Lewis dot structure (3) that an α-particle corresponds to a lone pair of electrons. For example, in $^{16}O_{c\text{-}2+2}{}^{4242}$, 2 dots and 2 lone pairs will identify with 2 d and 2 α; if 2 ^{1}H atoms descended on the 2 d extended lines, geometrical angle being 109.5° , it is a M-N structure of $^{1}H_2{}^{16}O$ (Fig. 2*B*). At near the 3rd layer end, nuclei begin to grow valence neutrons that first clearly to emerge 4 ^{v}n will be in $^{40}Ar_{v\text{-}4}$ in stable nuclei (~ 300), where the 4 ^{v}n position is to grow out 4 B α-clusters of next step.

2.3. The 4-5 periods: nuclear expansible core. Along with nuclear crystal growing to the 4th layer, its skin area will increase enough to hold another 4 B α-clusters (transition metals) in between 4 A α-clusters; further, in order to support increasing mass its core will be intensified in old group 8B. In terms of electron distributions, a proton distribution of $_{21}$Sc is 2 ^{l}p of $_{19}$K and $_{20}$Ca to float on 2 A axes, only the ^{l}p of $_{21}$Sc fit on B axis, but it seems to be questionable for nucleon arrangements of subsequent elements; i.e., the 3 ^{l}p of $_{19}$K, $_{20}$Ca and $_{21}$Sc should simultaneously glide upon B axes (^{40}Ar+b-111, ^{45}Sc, in later). However, it is hardly possible that protons like electrons is a probability distribution. In comparison, a pair distributions of electrons and protons is $_{21}$Sc-e(18)ds^2/p(18)d^3 (in proton distributions, A = s+p that in the range Z = 3-26, basal 2 p and 2 n which 4 A axes stand on have not been distinguished, B = d and C = f, respectively). Thus, from $_{19}$K to $_{26}$Fe in a total of 8 ^{l}p is piled on 4 B axes. The 2 ^{l}p of $_{27}$Co and $_{28}$Ni begin to sink into the core (Fig. 1*B*). The 2 ^{l}p of $_{29}$Cu and $_{30}$Zn will slip back upon A axes, though they are B family elements, then until to $_{36}$Kr, the 8 ^{l}p are piled on 4 A axes. The 5th layer is the same as the 4th layer, and, the 2 ^{l}p of $_{45}$Rh and $_{46}$Pd in groups 9-10B (Fig. 1*C* and figs. S45-46) have also been sunk into the core, which may be finished that a total of 6 ^{l}p (Z = 1, 2, 27, 28, 45 and 46) with 6 n are to form an innermost close-packed core (Fig. 2*A*).

Originally, here also felt puzzling that where the ^{l}p of $_{27}$Co should put on. Going through a period of time fiddling with its disorderly nucleon distribution, it seems to indicate that the ^{l}p of $_{27}$Co to put on the center is an optimal option due to ^{56}Fe skin closure, i.e., $^{56}Fe_{c\text{-}2+2}{}^{4444}$ (91.7%) → $^{59}Co_{c\text{-}4+3}{}^{4444}$ (100%) (Table 1 and figs. S26-27), $_{27}$Co-e(18)d^{7}s^2/p(19)d^8. First, it can explain a problem that why exist old group Fe-Co-Ni 8B in the periodic table. Second, this performance will enable a nucleus to possess a definite hub, a Coulomb repulsion center, otherwise its shape can not be opened up, however, like a tiny liquid drop (10). Parallel to this is in that a chart (13), per nucleon binding energy ~ 8.7 MeV is maximal, as nuclear mass increase to A ~ 60, i.e. Fe-Co-Ni region, which would imply that though at this region nuclear core has been intensified immediately, a sharp change of nucleon distributions, its curve remains to fall from Fe, a last element owning c-2+2. Additionally, ferromagnetic only occurs in Fe, Co and Ni at room temperature which possibly has a link to it, i.e. a structure and vibratory pattern of Fe, Co and Ni nuclei. However, the expansible core in nuclear growth show to be rather suitable, such as c-2+2 in ^{16}O, ^{40}Ca, c-4+4 in ^{60}Ni, ^{88}Sr and c-6+6 in ^{120}Sn, ^{208}Pb these magic nuclei (Table 1).

2.4. The 6-7 periods: folding nucleus. One of extraordinary feature in the periodic table is old group 8B existence, implying that nuclei contain a expansible core, the other is the number of inner transition metals, from where a particular place, $_{57}$La-e(54)ds^2/p(54)f^3, start to grow out between 4 A and 4 B α-clusters, implying that nuclei are folding. The extrapolation is that, if C family ^{l}p were fitting on 6 faces or 12 sides of Fig. 1*A*, it needs 12 ^{l}p or 24 ^{l}p, what is both impractical. Therefore, it should averagely vacate 4 sides in the 12 sides that only occupy 8 sides to grow 8 C α-clusters. On the other hand, whether C family contains 14 elements? If so, while assume that α is one of particles to construct a nucleus, as such an odd number of 7 α will be

asymmetric in a nuclear shape (coordinate). So far, it is thought that nuclear shapes might have not been so easy to recognize, whereas in here are tangible that nuclear shapes almost are tetrahedral in A step (^{12}C, ^{28}Si) and cubic in B step (^{74}Ge, ^{120}Sn), but in C step (^{208}Pb), the shape would be kept in a phase that between cubic and flat, which might result from a nuclear vibratory pattern that only allows to occur 8 C α-clusters. In fact, this nuclear pattern first is two dimensional using Go game stones to put on the floor (see also figs. S1-125), whereas it is so coincidental that when it is folded into three dimensional, such as ^{12}C, ^{74}Ge and ^{208}Pb (Fig. 2*A*). However, from the number of inner transition metals being 16 or 14, not other numbers, and valence neutron number (see below), it strongly suggests that a nuclear shape is folding, and, the heavier, the flatter; further, the extrapolation of C family 8 α-particles appears helpful to explain angle distribution of fission α-particle (section 4.5).

2.5. Vertical 16 α-clusters. As in Table 1, axial configurations of 16 α-clusters show to correspond to the groups that is almost the same in a big group, regardless of group A, B and C. For example, in big group 7 (7A, 7B, 13-14C), axial configuration 4443 is always found in ^{19}F, ^{35}Cl, ^{79}Br, ^{127}I of 7A, ^{55}Mn, ^{99}Tc, ^{193}Ir of 7B and ^{165}Ho$^{c\text{-}4443\text{-}4343}$, ^{166}Er$^{c\text{-}4443\text{-}4443}$ of 13-14C. In big group 3, a di-neutrons may often serve as a proton in skins of mid-heavy nuclei; e.g., ^{45}Sc$^{b\text{-}111\underline{2}}$ and ^{89}Y$^{b\text{-}111\underline{2}}$ in 3B, each of them has 3 ^{l}p to stay on 3 axes of 4 B axes, then a ^{d}n will substitute for a proton to occupy a surplus axis, thus, the 4 particles ($3^{l}p+1^{d}n$) are formed a stable b-tetrahedron out of their ^{m}c, i.e., ^{40}Ar+b-111$\underline{2}$ (^{45}Sc, 100%) and ^{84}Kr+b-111$\underline{2}$ (^{89}Y, 100%), similar to a b-tetrahedron of ^{40}Ar+b-2222 (^{48}Ti, 73.7%) that is different from an a-tetrahedron of such as ^{20}Ne+a-2222 (^{28}Si) (Table 1). In 3A occurs ^{69}Ga$^{a\text{-}111\underline{2}}$ and 5-6C occur ^{141}Pr$^{c\text{-}1010\text{-}111\underline{2}}$, ^{142}Nd$^{c\text{-}111\underline{2}\text{-}111\underline{2}}$. In stable nuclei, ^{45}Sc is likely emerging di-neutrons for the first time, which seems a unique structure. In group 1A, a ^{7}Li (92.5%) may prefer a-100 to a-3 (a single triton, alternative) in its skin, including below ^{23}Na^{100} (100%) and ^{39}K^{100} (93.3%), because skin particle masses will smoothly increase from 1 to 4 along with sweeping big groups from 1 (1A, 1B, 1C) to 8 (8A, 8-10B, 15-16C). In other words, nuclear skin may be thicker and thicker from left to right in the periodic table.

Evidently, there is a correspondence between the periodicity of atoms and nuclei that a nuclear axial configuration is repeated in every layer, such as a-4443 in ^{19}F (100%), ^{35}Cl (75.7%), ^{79}Br (50.6%) and ^{127}I (100%) in group 7A that all of their chemical main valence is 1. Perhaps, it cannot be excluded that the different physical and chemical properties of A, B and C three family elements are principal rooting in that A long, B mid and C short α-clusters extend a different depths in nuclei (Fig. 2*A*). Such as lanthanide contraction, it may be relevant to C family 16 ^{l}p trapped in 8 C axes where is low lying between 4 A and 4 B axes, implying that nuclear radii (14) might link to atomic radii (15). Using ^{23}Na^{35}Cl M-N structure (fig. S119) as an example, thin a-100 in ^{23}Na may be looser to the ^{m}c than thick a-4443 in ^{35}Cl, like that nucleon halo, if involved nuclear force; i.e., interstice between ^{m}c and ^{m}s in ^{20}Ne+a-100 (^{23}Na) is larger than in ^{20}Ne+a-4443 (^{35}Cl), a factor possible influence on their atomic radii (0.15 and 0.09 nm, respectively). However, it seems reasonable to conclude that the short 2-3, long 4-5 and very long 6-7 periods are to originate from nuclear 4 (A), 4+4 (A+B) and 4+4+8 (A+B+C) α-clusters standing on the expanding core (the very short 1 period), respectively. The vertical 16 α-clusters in Fig. 2*A* show to be bound with excess neutrons in nuclei that are valence neutrons in all probability.

3. Composition of beta stable line

3.1. Stable nuclei. A distinction between electron and proton distributions is proton distributions accompanied with neutrons. Generally in a nucleus neutrons exceed protons in number, as the slope of beta stable line (neutron-proton ratios) plotting in a chart (16), suggesting to derive from

$$A = Z + {}^{p}n + {}^{v}n, \qquad \textbf{[1]}$$

where ${}^{p}n$ is nearly the same as proton in number and distribution, and ${}^{v}n = 2(2^2, 2^3, 2^4)$ are valence neutron holes in A, B and C steps of crystal nuclei, respectively (Fig. 2*A*), e.g. ^{132}Xe = 54 + 54 + $2(2^2+2^3)$ in Table 1. As shown in Fig. 2*A*, a natural element (nucleus) at most comprise 40 ${}^{v}n$ derived from the 2-6 layers. In addition, in a nucleus ${}^{v}n$ approximates to α in number, e.g., ^{132}Xe = $24({}^{v}n+\alpha) + {}_{6}12$, where ${}_{6}12$ is its core in ${}_{Z}A$ ($Z = 6$, $A = 12$, its structure is very different from a ^{12}C); the ${}_{6}12$ might be replaced by a ${}_{6}18$ in ^{222}Rn (Table 1), even in ^{302}118 ($Z = 118$, fig. S118*B*), a 6n-6p-6n sandwich core.

Table 1 shows an interesting phenomenon that grown masses are an odd number in most cases. In particular, 1, 3, 1, 3, 1, 3 and 5 in the 3rd period, when grow from odd to even Z, only fill 1 ${}^{l}p$ (^{23}Na$^{100}\rightarrow{}^{24}$Mg^{1010}) or with 4 ${}^{v}n$ (^{35}Cl$^{4443}\rightarrow{}^{40}Ar_{v\text{-}4}{}^{4444}$), but 1 ${}^{l}p$ is often accompanied by 2 ${}^{p}n$ (^{28}Si$^{2222}\rightarrow{}^{31}$P^{4232}) from even to odd Z. Commonly, isotopic mass change for light nuclei was ${}^{p}n$ as ^{16,17,18}O in Fig. 2*B*. For mid nuclei, e.g., ^{112}Sn$_{v\text{-}12}{}^{2222}$ (0.96%) and ^{124}Sn$_{v\text{-}20}{}^{3333}$ (5.94%), both ${}^{p}n$ and ${}^{v}n$ were varied (Table 2).

In some cases this primary neutron fit is alternative. For example, a ^{36}S (0.014%) is ^{36}S$_{v\text{-}4}{}^{4242}$ (fig. S16*D*) or ^{36}S$_{v\text{-}2}{}^{4343}$ that how to balance ${}^{p}n$ and ${}^{v}n$, and 20 ${}^{v}n$ of ^{127}I is v-0,4,8,8 (fig. S53) or v-4,4,8,4 (Table 1) in the 2-5 layers. Perhaps, in a nucleus m,neutron different distributions are correlated with nuclear isomers (17) (marked m1, m2, m3…), while its proton frame is unconcerned; e.g., ^{79}Br$_{v\text{-}4,4}$ (50.69%) and ^{79m}Br$_{v\text{-}0,0,8}$ (5.1 s), its inner 8 ${}^{v}n$ would be excited to outer (figs. S35*A-B*), or other distributions in the 2-4 layers (also see ^{119m,121m}Sn in Table 2). For nuclei, however, figs. S3*A*-18*C* indicate that: the higher is the abundance (half-life), the more concise is the structure, such as ^{12}C^{2222} (98.93%), ^{13}C^{3222} (1.07%), ^{14}C^{3232} and ^{28}Si^{2222} (92.223%), ^{29}Si^{3222} (4.685%), ^{30}Si^{3232} (3.092%).

3.2. Unstable nuclei. Away from the beta stable line, due to $Z > N$, ^{3}He was estimated to generate in skin of neutron-deficient light nuclei, e.g. ^{19}Ne$_{c\text{-}2+2}{}^{4443}$ (17.22 s) and ^{17}Ne$_{c\text{-}2+2}{}^{4333}$ (109.2 ms). Furthermore, a heavy nucleus lack of neutrons, ${}^{v}n$, to bind its vertical A-5α, B-3α and C-1α clusters may more easily cause decay (emission) (18, 19), corresponding to the fact that α-decay only happen in neutron-deficient heavy nuclei (in mid nuclei almost never, e.g. $^{99\text{-}111}$Sn isotopes in Table 2) that begin to grow C-1α clusters, where also most likely is a point of fission α-particle (Fig. 2*A*). To some extent, both α and cluster decay seem to result from the 16 α-clusters cleft into 15:1 similar to nuclear fission that only cleft ratios are different (Table 3).

For neutron-rich nuclei, e.g., a structure of superlarge ^{11}Li-$^{2}1^{2}$,$2^{a\text{-}2000}$,3^{00} (8.75 ms) was a ${}^{m}c$ of ^{9}Li with a 2 neutron halo (20). Additionally, a neutron skin (halo) may happen in a stable nucleus; e.g., ^{136}Xe-$^{6}1^{6}$,$^{8}4^{8}$,$^{8}4^{8}$,$^{16}8^{16}$,$^{16}8^{16}$,6^{0000} (8.9%), this 4 n (6^{0000}) skin will cage a ^{132}Xe, because its ${}^{p}n$ and ${}^{v}n$ shells are closed.

Note that, unexpectedly, all of Z , ${}^{p}n$ and ${}^{v}n$ three shells closed ($A = 2Z + {}^{v}n$, ideal nucleus) shows not a most stable structure from two abundance (half-life) lines of ideal nuclei and their maximal abundant isotopes (Table 1) intersecting at ^{132}Xe$_{v\text{-}4,4,8,8}$ (26.9%), i.e., for ideal nuclei, ${}^{v}n$ too many in ^{24}Ne$_{v\text{-}4}$ (3.38 min), ^{44}Ar$_{v\text{-}4,4}$ (11.87 min) and ^{88}Kr$_{v\text{-}4,4,8}$ (2.84 h), but too few in ^{212}Rn$_{v\text{-}4,4,8,8,16}$ (23.9 min). Nevertheless, here was unable to find a better way to fit pair and valence neutrons with the line of beta stability. In the followings, it is therefore probably not surprising that valence neutrons prevail over pair neutrons to become released neutrons in fission.

Table 2. A tentative arrangements of $^{99\text{-}138}$Sn.

Commonly, in these 39 neutrons (138 - 99), ^{v}n ~ 21, ^{p}n ~ 8, and 10 n in the 6th layer is neutron skin (halo), meaning that Sn isotopes might only grow ^{v}n from $A > {}^{120}$Sn. All of valence neutrons in the 2-6 layers is compiled in a column. Decay modes: ε, electron capture; p, proton emission; IT, isomeric tranition; β^-, beta-minus decay; n, neutron emission.

Sn isotope	core+middle	valence neutron	axial configuration		abundance (%) / half-life (decay mode)
99	76	0, 0, 3	b-4444	a-1111	
100	-	0, 0, 4	-	1111	0.86 s (ε, εp)
101	-	0, 0, 5	-	-	1.7 s (ε, εp)
102	-	0, 0, 6	-	-	3.8 s (ε)
103	-	0, 0, 7	-	-	7.0 s (ε, εp)
104	-	0, 0, 8	-	-	20.8 s (ε)
105	-	0, 0, 8	-	2111	32.7 s (ε, εp)
106	-	0, 0, 8	-	2211	115 s (ε)
107	-	0, 0, 8	-	2221	2.90 min (ε)
108	-	0, 0, 8	-	2222	10.30 min (ε)
109	-	0, 1, 8	-	-	18.0 min (ε)
110	-	0, 2, 8	-	-	4.11 h (ε)
111	-	0, 3, 8	-	-	35.3 min (ε)
112	-	0, 4, 8	-	-	0.96
113	-	0, 4, 8	-	3222	115.09 d (ε)
114	-	0, 4, 8	-	3322	0.66
115	-	0, 4, 8	-	3332	0.34
116	-	0, 4, 8	-	3333	14.54
117	-	1, 4, 8	-	-	7.68
118	-	2, 4, 8	-	-	24.22
119	-	3, 4, 8	-	-	8.59
119m	-	4, 4, 8	-	3332	291.1 d (IT)
120	-	4, 4, 8	-	3333	32.58
121	-	4, 4, 8, 1	-	-	27.03 h (β^-)
121m	-	3, 4, 8, 2	-	-	43.9 yr (IT)
122	-	4, 4, 8, 2	-	-	4.72
123	-	4, 4, 8, 3	-	-	129.2 d (β^-)
124	-	4, 4, 8, 4	-	-	5.94
125	-	4, 4, 8, 5	-	-	9.64 d (β^-)
126	-	4, 4, 8, 6	-	-	2.3×10^5 yr
127	-	4, 4, 8, 7	-	-	2.10 h (β^-)
128	-	4, 4, 8, 8	-	-	59.07 min (β^-)
129	-	4, 4, 8, 8, 1	-	-	6.9 min (β^-)
130	-	4, 4, 8, 8, 2	-	-	3.72 min (β^-)
131	-	4, 4, 8, 8, 3	-	-	56.4 s (β^-)
132	-	4, 4, 8, 8, 4	-	-	39.7 s (β^-)
133	-	4, 4, 8, 8, 5	-	-	1.46 s (β^-, β^-n)
134	-	4, 4, 8, 8, 6	-	-	1.05 s (β^-, β^-n)
135	-	4, 4, 8, 8, 7	-	-	530 ms (β^-, β^-n)
136	-	4, 4, 8, 8, 8	-	-	0.25 s (β^-, β^-n)
137	-	4, 4, 8, 8, 9	-	-	190 ms (β^-, β^-n)
138	-	4, 4, 8, 8, 10	-	-	~ 408 ns

4. Fission configuration

As fission can direct reflect details of a nuclear structure, there is an attempt to depict it to test the crystal model; at this stage that fission configuration remains poorly understood a brief depiction may be more effective. Generally, nuclei can occur asymmetric and symmetric fission (21-23, 28-35). Asymmetric fission shows peaking to $Z = (86+102) / 2 = 94$ in thermal neutron (n,f) and spontaneous (sf) fission, where 86 and 102 are A and C closed shells, implying that it may only occur within the two shells. Its process is possible that: when a neutron land on a nuclear skin and induce its skin particles to glide, more or less, to the one side, or from side to side repeatedly, then the nucleus would be cleft, likely in that when its shape is just unfolded and thus its cleft place is a line to emit neutrons, somewhat similar to a crystal cleft. If increase excitation energy, its skin particles have insufficient time to glide and its core, a relatively firm six neutron center, might be broken up, thus a symmetric fission will happen. Accordingly, the core, middle and skin of a folding crystal nucleus may play different parts in fission.

Table 3. Some fission types and paths of ^{236}U.

Fission type (different divide of core $_6$12 nucleons) was mainly classified into: 1/2, $_3$6:$_3$6; 1/4, $_3$3:$_3$9; 0, 0:$_6$12. The $^{\nu}$n number error is about $\pm$3 in mass division, which could be related to isotopic products. Skin nucleons and valence neutrons in the cleft lines have not been allotted to α-cluster decay.

fission type and path	cleft ratio of 16 α-clusters	*Z*-*A* distribution A_L	A_H
1-1/2-9	$2^a2^b4^c : 2^a2^b4^c$ (8 : 8)	^{118}Pd	^{118}Pd
2-1/2-9	$2^a2^b3^c : 2^a2^b5^c$ (7 : 9)	^{111}Tc	^{125}In
3-1/2-9	$2^a1^b3^c : 2^a3^b5^c$ (6 : 10)	^{95}Rb	^{141}Cs
4-1/2-9	$2^a1^b2^c : 2^a3^b6^c$ (5 : 11)	^{88}Se	^{148}Ce
1-1/4-8	$1^a2^b4^c : 3^a2^b4^c$ (7 : 9)	^{94}Kr	^{142}Ba
2-1/4-8	$1^a2^b3^c : 3^a2^b5^c$ (6 : 10)	^{85}As	^{151}Pr
3-1/4-8	$1^a1^b3^c : 3^a3^b5^c$ (5 : 11)	^{69}Co	^{167}Tb
4-1/4-8	$1^a1^b2^c : 3^a3^b6^c$ (4 : 12)	^{60}Cr	^{176}Er
1-0-9	$2^a2^b4^c : 2^a2^b4^c$ (8 : 8)	^{112}Tc	^{124}In
2-0-9	$2^a2^b3^c : 2^a2^b5^c$ (7 : 9)	^{105}Zr	^{131}Te
3-0-9	$2^a1^b3^c : 2^a3^b5^c$ (6 : 10)	^{89}Se	^{147}Ce
4-0-9	$2^a1^b2^c : 2^a3^b6^c$ (5 : 11)	^{82}Ga	^{154}Pm
α-cluster decay			
1-0-2	1^c : $4^a4^b7^c$ (1 : 15)	^{4}He	^{232}Th
2-0-3	1^b : $4^a3^b8^c$ (1 : 15)	^{12}C	^{224}Rn
4-0-5	1^a : $3^a4^b8^c$ (1 : 15)	^{20}Ne	^{216}Pb

4.1. Fragment structures. On the whole, fragment charge and mass is a statistical distribution. In Fig. 2*A* it appears to come from 16 α-clusters of a nucleus cleft into different ratios (colonies, Table 3), in which asymmetric fission is a double peak yield curve (21-23) that a contribution of skin particle glide might be involved. As a shift ratio of ^{m}s is a random distribution at present, while ^{m}c (^{212}Rn^{4444}, fig. S86*A*, ^{208}Pb^{3333}+4^{l}p, Fig. 2*A*) has several fixed divisions, a fission system ($_Z$*A* > ^{212}Rn) is resolved: X = ^{m}c + ^{m}s. Thus, a fragment often is a mixture of ^{m}c and ^{m}s. For example, in 1-1/4-8 fission of ^{235}U+n, a structure of ^{235}U being ^{6}1^6,$^8_4$2^8,$^8_4$3^8,$^{16}_8$4^{16},$^{16}_8$5^{16},$^{32}_{16}$6^{32},7$^{a\text{-}0000,b\text{-}0000,c\text{-}2222\text{-}2220}$, its ^{m}c is lined off:

$$^{212}\text{Rn}_{\text{ 1-1/4-8}} \rightarrow {}_{53}129 + {}_{33}83, \quad \textbf{[2]}$$

where subscript is fission path that its image is somewhat analogous to a tetrahedron cutting off an angle (1 A axis, 3:1, $3^a2^b4^c$:$1^a2^b4^c$) nearby center, and its ^{m}s falls into

$$\text{a-000,b-00,c-222}\underline{2} + \text{a-0,b-00,c-222}\underline{2} = {}_3 13 + {}_3 11, \quad \textbf{[3]}$$

a total of 24 nucleons on the skin including a thermal neutron; then add Eq. 3 to Eq. 2,

$$^{235}\text{U+n}_{\text{ 1-1/4-8}} \rightarrow ({}_{53}129+{}_3 13) + ({}_{33}83+{}_3 11) = {}^{142}\text{Ba} + {}^{94}\text{Kr}, \quad \textbf{[4]}$$

$$^{235}\text{U+n}_{\text{ 1-1/4-8}} \rightarrow {}_{53}129 + ({}_{33}83+{}_6 24) = {}^{129}\text{I} + {}^{107}\text{Y}, \quad \textbf{[5]}$$

$$^{235}\text{U+n}_{\text{ 1-1/4-8}} \rightarrow ({}_{53}129+{}_6 24) + {}_{33}83 = {}^{153}\text{Pr} + {}^{83}\text{As}, \quad \textbf{[6]}$$

that is, when $_3$13 glide into 1-8 sector [5] or $_3$11 into 8-1 sector [6], they are ^{107}Y (94+13) or ^{153}Pr (142+11), suggesting that a fragment peak yield (28-31) may be partly contributed from $_3$13 and $_3$11 glide. In Eq. 4 ^{m}s has not glided that two fragment peak yields are near 6%. The valley is a symmetric fission:

^{235}U+n $_{1\text{-}1/2\text{-}9}$ → $_{46}$118 + $_{46}$118, **[7]**

near 0.1% yield.

4.2. Fragment mass difference. Between two fragments, a mass difference can be setting up by a single C, B or A axis (Table 3). To an A axis, it is, e.g.,

^{235}U+n $_{1\text{-}1/2\text{-}8}$ → ($_{53}$126+$_3$13) + ($_{33}$86+$_3$11) = ^{139}Ba + ^{97}Kr = ($_{46}$118+$_{10}$21) + ($_{46}$118 - $_{10}$21), **[8]**

where $_{10}$21 = $_{10}$20 + 1, a cluster of 5 α (A3 axis) plus 1 n at A3-7 position, when the cleft line sweep anticlockwise from 1-1/2-9 [7] to 1-1/2-8.

4.3. Fragment vanishing points. Fragment yields, including of A_H, A_L (22), neutron (24, 25, 36) and α-particle (21), show to vanish in the same two points at leftmost sides of double mass peaks, ~ 130 and ~ 80, which both suggest to come from an α-cluster colony where its 2 edges are enclosed by long 2 A axes, i.e., $3^a2^b4^c$ (A_H, e.g. 8-1 sector) and $2^a1^b2^c$ (A_L, e.g. 4-9 sector) α-cluster colonies. Take neutron yields for example, in

^{252}Cf $_{1\text{-}1/4\text{-}8}$ → $_{53}$129 + ($_{33}$83+$_{12}$40) = $_{53}$129 + $_{45}$123, **[9]**

where $_{53}$129 is a minimal $3^a2^b4^c$ colony, and $_{45}$123 is a complementary colony ($1^a2^b4^c$) to yield maximal neutrons (~3) (24), suggesting that maximal neutron yield is from a sector of short 2 C axis edges. In ^{254}Fm (sf) that both ^{252}Cf and ^{254}Fm neutron shells were ^{p}n-114+^{v}n-40 shows a similar result of neutron yield: minimum at 129-130 of A_H and maximum at 123-124 of A_L (36). In 4-0-9 fission, there is

^{252}Cf $_{4\text{-}0\text{-}9}$ → ($_{56}$142+$_9$28) + ($_{30}$70+$_3$12) = ^{170}Tb + ^{82}As, **[10]**

which is an extreme event that $2^a1^b2^c$+$_3$12 (^{82}As) has not held any ^{v}n in the cleft line. Similarly, a neutron deficient fragment seems also in the vicinity of an enclosed $3^a2^b4^c$ or $2^a1^b2^c$ colony. For instance, in ^{238}U+^{12}C (35), a $^{73}_{33}$As likely come from $_{30}$70+$_3$3 in 4-1/4-9 fission, where $_{30}$70 = 5α × 2+3α+1α × 2+10^{v}n, a minimal $2^a1^b2^c$ colony, and $_3$3 is from core. For ^{72}As and ^{69}Zn in ^{238}U+p (37), they might come from other ways, such as a $1^a2^b2^c$ colony, because the 10 ^{v}n normally cannot be released inside a minimal $2^a1^b2^c$ colony ($^{70}_{30}$Zn) (35), unless one of them has become a delayed neutron (38), when the fragment was reconstituted to turn into a daughter nucleus. However, it implies that no matter what is prompt (from a fragment edges) or delayed (from a fragment middle) neutrons, both them come from valence neutrons in most cases.

4.4. Skin particle glide. Comparing Eq. 5 and Eq. 6 suggests that ^{m}s prefer to glide upon the top of A_L ($3^a2^b4^c$:$1^a2^b4^c$+^{m}s), for the yield of Eq. 5 is usually higher than Eq. 6. This view is also illustrated by that A_H masses are nearly constant, while A_L masses increase in ^{229}Th, ^{233,235}U, ^{239}Pu, ^{245}Cm, ^{249}Cf and ^{254}Es (n,f) (22). However, particles in skin may glide limited in the two closed shells that transition from asymmetry to symmetry is in two sides of Z 94±6 ($_{88}$Ra-$_{100}$Fm) (39), implying that its mass number is neither too many, nor too few. For example, in the light side there is ^{226}Ra (^{3}He, df) that simultaneously reveal asymmetric and symmetric fission (40). In the heavy side, transition is in Fm isotopes (36, 39, 41-43), which from $^{254}_{100+114+40}$Fm$^{a\text{-}0000,b\text{-}\underline{2222},c\text{-}4443\text{-}4443}$ (sf, asymmetric) to $^{258}_{100+118+40}$Fm$^{a\text{-}\underline{2222},b\text{-}\underline{2222},c\text{-}4443\text{-}4443}$ (^{257}Fm+n, symmetric), a-0000 was replaced by a-2222 at the top of 4 A axes (see superscript and subscript). This is likely that the closed ^{p}n-118 shell (see also fig. S100) fence against the skin particles to glide and drive a ^{258}Fm bisected. In the case of $^{252}_{102+110+40}$No$^{a\text{-}0000,b\text{-}0000,c\text{-}4444\text{-}4444}$, though its Z-102 shell is closed (see also fig. S102), it is an asymmetric fission (44), possible that it lack 8 ^{p}n than ^{258}Fm in the skin to resist the ^{m}s glide.

Possible to result in even-Z fragment that its energy release is greater than odd (fine structure of fragment masses, interval A ~ 5, ^{v}n+α) (28-31), part of skin particles might be fused in glide, since in ^{235}U (n,f), its skin having no an inherent α-particle in ground state, has occurring polar α-particle emission, about 0° or 180° with respect to the fission axis, and, over 3 times for A_L to A_H flight directions (45-47), which is in favor of ^{m}s to glide upon A_L also. In order to clarify

whether polar emission come from ^{m}s glide, if possible, could try to detect that symmetric fission; e.g. ^{208}Pb (Fig. 2*A*) or ^{257}Fm (n,f), their ^{m}s are almost unable to glide and estimate that polar emission is less than ^{235}U (n,f).

4.5. Ternary fission, α and cluster decay. Binary fission in Fig. 2*A* could draw a line from one side through the core to the opposite side. When draw three lines, e.g., 1-c (from N1-6 to core), 2-c and 9-c. it is a ternary 1-2-9 fission. Usually, 1-2 sector (one of 8 C axes) is a place of light charged particle (LCP) emission (21, 26, 27, 48, 49) and can partition it into three points: C1-7 (p, d, t, α), C1-6 (α) and C1-6+C1-7 (^{7,8,9}Li, ^{9,10}Be). Among them most probable emission is α and its angle to differ from polar emission is perpendicular to the fission axis, nearly 90±22.5° to A_H and A_L, respectively, where 22.5° = 360°/16. Since a fission nucleus is almost impossibly complete unfolded, its α emitting angle is within 67.5° -112.5°, which is in good agreement with results reported (26, 27) that is difficult to explain up to now, to the author's knowledge. In addition, it is possible that LCP, just in the two ends of a cleft line, could serve as a probe to identify axial configurations on the condition that ^{m}s has not glided or in glide $_{Z}A$ of some LCP have not varied. LCP emission probabilities in per 10^3 sf of ^{252}Cf$^{a\text{-}0000,b\text{-}\underline{2222},c\text{-}4343\text{-}4343}$ are: α-3.3, t-0.2, d-0.02 and p-0.06, respectively (48), slightly less than ideal that its axial configuration has 4 α and 4 t, no d and p.

If the track varied from 1-2-9 to 1-4-8 randomly, it is a three large fragment fission (50, 51), in which ^{235}U (n,f), three sectors are about 1-4 (^{35}Mg), 4-8 (^{56}Sc) and 8-1 (^{145}Pr). It therefore suggests that lighter fragments, including α-cluster decay, most likely result from a different combination of A, B and C axes, e.g., 1^{c}, $A \sim 10$, LCP; $1^{b}2^{c}$, $A \sim 30$, ^{28}Mg (51); $1^{a}1^{b}1^{c}$, $A \sim 50$, ^{47}Ca, ^{48}Sc (37). From here, it is tempting to expect that a nucleus might deeply be fragmented into four large fragments; e.g., in a quaternary 1-3-9-14 fission of ^{235}U+n, four sectors are 1-3 (^{25}F), 3-9 (^{93}Rb), 9-14 (^{69}Co) and 14-1 (^{49}K). However, four coincident fragment angular, energy and mass as a function of excitation energy in a quaternary fission would shed intriguing light upon that whether a nuclear shape is from folded (tetrahedral 4 A axes) to unfolded (plane 4 A axes) in fission.

5. Discussion

Here, it has described that folding crystal of nuclei can grow vertical 16 α-clusters of different length bound with valence neutrons to stand the core. In fission, some of ^{v}n in a cleft line will convert into free neutrons and give rise to 16 α-clusters cleft, like a molecular bond broken, into symmetric 8:8, or asymmetric 9:7 (Fig. 2*A*) that its a pair fragment mass difference is about 5 α × 2 = $_{20}$40 (±1 A axis, 2 clusters of 5 α), which is well consistent with data obtained (21-23), for a typical example, ^{235}U+n→^{137}Ba+^{97}Kr+2n.

To explain why two coincident fragments have a characteristic mass difference is a crucial problem in nuclear fission. Sometimes, a heavy fragment was explained near *Z*-50, *N*-82 doubly magic shells (41) and a light fragment near *N*-50 shell (21), which seem that a clear distinction between solid structures of proton and neutron shells has not been made. Likely, their shells are the same only in magic number 2 (^{4}He), 8 (^{16}O) and 20 (^{40}Ca) (Table 1); for the 28, 50 and 82, it is to differ because of valence neutron emergence, suggesting that proton shells are constant, whereas neutron shells are not in a number. For example, *Z*-50 shell is all along fixed, when isotope mass increasing from $^{99}{}_{50+46+3}$Sn to $^{138}{}_{50+54+34}$Sn (Table 2), while *N*-50 shell has largely been changed that ^{v}n are gradually turned into ^{p}n to pair increased ^{l}p, when isotone charge increasing from $^{82}{}_{32+36+14}$Ge to $^{100}{}_{50+46+4}$Sn. However, it is likely different that *N*-50 shell in ^{88}Sr (^{84}Kr+a-1010) from ^{89}Y (^{84}Kr+b-11$\underline{12}$), *N*-82 shell in ^{138}Ba from ^{139}La, ^{140}Ce, ^{141}Pr and ^{142}Nd (Table 1). For that *N*-126 shell, in Fig. 2*A* shows to derive from ^{p}n-86+^{v}n-40, a frame to grow $^{208}{}_{82+86+40}$Pb^{3333}, ^{209}Bi^{4333}, ^{210}Po^{4343}, ^{211}At^{4443} and $^{212}{}_{86+86+40}$Rn^{4444}. Though only *Z*-2, *N*-2, *Z*-28 and *N*-126 shells are closed here (even if completely closed ideal nuclei are not most stable, except $^{132}{}_{54+54+24}$Xe), magic nuclei have encouragingly been displayed a definite images (Figs. 2*A-B*), and, it is undeniable that all magic nuclei together with their neighbor nuclei able to grow is so smooth in Table 1, which would be useful to account for magic number phenomena in the future.

On the other hand, it is not impossible that a nucleus might emerge different structures in ground and excited states. For example, a ^{16}O in ground state is $^{16}O_{c\text{-}2+2}{}^{4242}$ and in excited state is 4 α-structure (9) that skin 2 d of $^{16}O_{c\text{-}2+2}{}^{4242}$ were combined 1 α; otherwise in ground state how a 4 α-structure of ^{16}O can carry two hydrogen atoms to build a water molecule? Whereas a $^{1}H_2{}^{16}O$ M-N structure will have understood at a glance in Fig. 2*B*, suggesting that the action of a nucleus in a molecule might have to take into account (52). However, a compelling relation between light nuclei and simple molecules may have been carried out in this work, to some extent, which is an integrative result of alpha-particle model (9) plus valence neutrons and Lewis dot structure (3) (Table 1 and figs. S119-125). In addition to electron distributions, obviously, atomic scope was broadened to proton distributions significantly, though not to incorporate them. As the proton is predominant in an atom in a sense, the element properties may essentially result from the proton, *Z*, the atomic number, which is shown to occupy constant spatial positions not only in nuclei, but also in molecules as well (Fig. 2*B*), implying that the periodic law interpreted by proton might be less complicated, that is, the proton arrangements in nuclei are likely identical to the element arrangements in the periodic table (Figs. 1*A-C*).

Accordingly, the periodic law seems able to dominate structures of not only molecules and atoms (2-4), but nuclei (5, 6). Further, this nuclear crystal model appears to be feasible in depicted typical fission phenomena. Namely, a nuclear crystal fission is likely that its 16 α-clusters are cleft into different ratios from 15:1 (1^c, α decay; 1^b or 1^a, cluster decay, essentially similar to three large fragments in a fission) to 8:8 that a most probable ratio is 9:7 ($3^a2^b4^c$:$1^a2^b4^c$) and its charge and mass difference is ${}_ZA \geqslant {}_{20}40$ in two coincident fragments, released neutrons mostly come from valence neutrons, α-particle angle within $90 \pm 22.5^\circ$ to its fission axis is emitting from one of C family 8 α-particles, and, all fragment, neutron and α-particle yields suggests to vanish in the same two points: $3^a2^b4^c$ ($A_H \sim 130$) and $2^a1^b2^c$ ($A_L \sim 80$) α-cluster colonies (Fig. 2*A*) (21-27). Taken together, however, there is a fascinating possibility that the periodic table shape is rooting in nuclei that can only grow 1 α-particle in the 1st layer (core) intensified by 4 ^1p of ${}_{27}Co$, ${}_{28}Ni$, ${}_{45}Rh$ and ${}_{46}Pd$, and 2^3, 2^4 and 2^5 α-particles together with nearly same number valence neutrons in the 2-3, 4-5 and 6-7 layers, respectively (Fig. 2*A*), which is in general agreement with the line of beta stability. Consequently, the atomic number of the 1-7 periods is derived from Z $118 = 2(1+2^3+2^4+2^5) + 4$ that noble nuclei are able to demonstrate perfect nucleon distributions (Table 1) in three dimensions. Furthermore, the number of the elements [$2(2^3+2^4+2^5)$ besides groups 9-10B] and valence neutrons ($2^3+2^4+2^5$) in the A, B and C steps being a square relation therefore indicates that an element nucleus unusually is a two dimensional structure in a nuclear phase, a folding crystal plate of nucleons; so that gives rise to it, a crude nucleon aspect was suggested from macrocosm. However, though here is an empirical nucleon distribution, it provides a promising way that may be beneficial to further clarify and/or integrate nuclear, atomic and molecular structures.

Acknowledgments

This work was partly supported by Changzhou Bureau of science and technology, China. The author thanks Mr. Benlin Liu for an appreciation.

Supporting figs. S1-125 (154 photos, 35 MB)

References

1. Thomson JJ (1897) Cathode rays. *Phil. Mag.* **44**, 293.
2. Bohr N (1913) On the constitution of atoms and molecules. *Phil. Mag.* **26**, 476-502.
3. Lewis GN (1916) The atom and the molecule. *J. Am. Chem. Soc.* **38**, 762-785.
4. Langmuir I (1919) The arrangement of electrons in atoms and molecules. *J. Am. Chem. Soc.* **41**, 868-934.
5. Moseley HGJ (1913) The high frequency spectra of the elements. *Phil. Mag.* **26**, 1024.
6. Moseley HGJ (1914) Atomic models and x-ray spectra. *Nature* **92**, 554-554.
7. Rutherford E (1911) The scattering of α and β particles by matter and the structure of the atom. *Phil. Mag.* **6**, 21.
8. Chadwick J (1932) Possible existence of a neutron. *Nature* **129**, 312.
9. Hafstod LR, Teller E (1938) The alpha-particle model of the nucleus. *Phys. Rev.* **54**, 681.
10. Bohr N, Wheeler JA (1939) Phys. Rev. **56**, 426.
11. Haxel O, Jensen JHK, Suess HE (1949) On the "magic numbers" in nuclear structure. *Phys. Rev.* **75**, 1766.
12. Hahn O, Strassmann F (1939) *Naturwiss.* **27**, 89.
13. Friedlander G, Kennedy JW, Macias ES, Miller JM (1981) *Nuclear and Radiochemistry* (John Wiley & Sons, New York), p. 27.
14. Geiger H, Marsden E (1909) On a diffuse reflection of the α-particles. *Proc. Roy. Soc.* A **82**, 495-500.
15. Meyer JL, redrawn by Bayley T (1882) Phil. Mag. **13**, 26-37.
16. Bohr A, Mottelson BR (1969) *Nuclear Structure* (Benjamin, New York), vol. **1**.
17. Hahn O (1921) *Naturwiss.* **9**, 84.
18. Rose HJ, Jones GA (1984) A new kind of natural radioactivity. *Nature* **307,** 245-247. doi: 10.1038/307245a0.
19. Andreyev AN et al. (2013) Signatures of the Z = 82 shell closure in α-decay process. *Phys. Rev. Lett.* **110**, 242502. doi: 10.1103/PhysRevLett.110.242502.
20. CERN (2004) *"ISOLDE goes on the trail of superlatives". CERN Courier* May 4.
21. Schmitt HW, Neiler JH, Walter FJ, Chetham-Strode A (1962) Mass distribution and kinetics of ^{235}U thermal-neutron-induced three-particle fission. *Phys. Rev. Lett.* **9**, 427-429.
22. Unik JP et al. (1973) Fragment mass and kinetic energy distributions for fissioning systems ranging from 230 to 256. *Proc. IAEA Symp. Phys. Chem. Fission*, **2**, 19-46.
23. Dickens JK, McConnell JW (1986) Yields of fission products produces by thermal-neutron fission of ^{243}Cm. *Phys. Rev.* C **34**, 722-725.
24. Bowman HR, Milton JCD, Thompson SG, Swiatecki WJ (1963) Further studies of the prompt neutrons from the spontaneous of ^{252}Cf. *Phys. Rev.* **129**, 2133-2147.
25. Terrell J (1965) Prompt neutrons from fission. *Proc. IAEA Symp. Phys. Chem. Fission*, **2**, 3-24.
26. Fraenkel Z, Thompsom SG (1964) Properties of the alpha particles emitted in the spontaneous of ^{252}Cf. *Phys. Rev. Lett.* **13**, 438-441.
27. Fluss MJ, Kaufman SB, Steinberg EP, Wilkins BD (1973) Angular distribution in the spontaneous fission of ^{252}Cf. *Phys. Rev.* C **7**, 353-364.
28. Thomas TD, Vandenbosch R (1964) Correlation of fission-fragment kinetic-energy fine structure with a semiempirical surface. *Phys. Rev.* **133**, B976-982.
29. Reisdorf WN, Unik JP, Glendenin LE (1973) Correlation between fragment mass-distribution fine structure, charge distribution and nuclear structure for thermal-neutron-induced fission of ^{233}U and ^{235}U. *Nucl. Phys.* A**205**, 348-362.

30. Schmitt HW, Neiler JH, Walter FJ (1966) Fragment energy correlation measurements for ^{252}Cf spontaneous fission and ^{235}U thermal-neutron fission. *Phys. Rev.* **141**, 1146-1160.

31. Neiler JH, Walter FJ, Schmitt HW (1966) Fission-fragment energy-correlation measurements for the thermal-neutron fission of ^{239}Pu and ^{241}Pu. *Phys. Rev.* **149**, 894-905.

32. Plasil F, Ferguson RL, Pleasonton F (1973) Neon-induced fission of silver. *Proc. IAEA Symp. Phys. Chem. Fission*, **2**, 319-333.

33. Wilkins BD et al. (1984) Mass and kinetic energy distribution in near-barrier fission of ^{182}W. *Phys. Rev.* C **30**, 1228-1232.

34. Hulet EK et al. (1986) Bimodal symmetric fission observed in the heaviest elements. *Phys. Rev. Lett.* **56**, 313-316.

35. Delaune O et al. (2013) Isotopic yields distributions of transfer- and futon-induced fission from ^{228}U + ^{12}C reactions in inverse kinematics. *Phys. Rev.* C **88**, 024605. doi: 0.1103/PhysRevC.88.024605.

36. Gindler JE, Flynn KF, Glendenin LE, Sjoblom RK (1977) Distribution of mass, kinetic energy and neutron yield in the spontaneous of ^{254}Fm. *Phys. Rev.* C **16**, 1483-1491.

37. Klingensmith DL, Porile NT (1988) Fragment emission in the interaction of ^{238}U with 400 Gev protons. *Phys. Rev.* C **38**, 818-831.

38. Amiel S (1969) Delayed neutrons in fission. *Proc. IAEA Symp. Phys. Chem. Fission*, 569-590.

39. Ragaini RC, Hulet EK, Lougheed RW, Wild J (1974) Symmetric fission in the neutron-induced fission of ^{255}Fm. *Phys. Rev.* C **9**, 399-406.

40. Konecny E, Specht HJ, Weber J (1973) Symmetric and asymmetric fission of Ra- and Ac-isotopes. *Proc. IAEA Symp. Phys. Chem. Fission*, **2**, 3-18.

41. Balagna JP, Ford GP, Hoffman DC, Knight JD (1971) Mass symmetry in the spontaneous fission of ^{257}Fm. *Phys. Rev. Lett.* **26**, 145-148.

42. John W, Hulet EK, Lougheed RW, Wesolowski JJ (1971) Symmetric fission in thermal-neutron-induced and spontaneous fission of ^{257}Fm. *Phys. Rev. Lett.* **27**, 45-48.

43. Flynn KF, Gindler JE, Glendenin LE (1975) Distribution of mass in thermal-neutron-induced fission of ^{257}Fm. *Phys. Rev.* C **12**, 1478-1482.

44. Bemis CE et al. (1977) Fragment-mass and kinetic-energy distributions from the spontaneous fission of ^{252}No. *Phys. Rev.* C **15**, 705-712.

45. Piasecki E, Dakowski M, Krogulski T, Tys J, Chwaszczewska J (1970) Evidence of the polar emission of alpha-particles in the thermal neutron fission of ^{235}U. *Phys. Lett.* **33**B, 568-570.

46. Piasecki E, Dakowski M, Kordyasz A (1973) Recent studies on polar emission. *Proc. IAEA Symp. Phys. Chem. Fission*, **2**, 383-388.

47. Piasecki E, Nowicki L (1979) Polar emission in fission. *Proc. IAEA Symp. Phys. Chem. Fission*, **2**, 193-221.

48. Wild JK et al. (1985) Light-charged-particle emission in the spontaneous fission of ^{250}Cf, ^{256}Fm and ^{257}Fm. *Phys. Rev.* C **32**, 488-495.

49. Wagemans C, D'hondt P, Schillebeeckx P, Brissot R (1986) Triton and alpha emission in the thermal-induced ternary fission of ^{233}U, ^{235}U, ^{239}Pu and ^{241}Pu. *Phys. Rev.* C **33**, 943-953.

50. Muga ML, Rice CR, Sedlacek A (1967) Ternary fission of heavy nuclei. *Phys. Rev. Lett.* **18**, 404-408.

51. Iyer RH, Cobble JW (1966) Evidence of ternary fission at lower energies. *Phys. Rev. Lett.* **17**, 541-545.

52. Yixing C et al. (2016) Electrolytes induce long-range orientational order and free energy changes in the H-bond network of bulk water. *Science Advances.* Vol. **2**, no. 4, e1501891. doi: 10.1126/sciadv.1501891.